Bolton, M. D. & Wilson, J. M. R. (1989). *Géotechnique* **39**, No. 4, 585–599

An experimental and theoretical comparison between static and dynamic torsional soil tests

M. D. BOLTON* and J. M. R. WILSON*

The dynamic properties of dry Leighton Buzzard sand have been investigated using a resonant column test apparatus. These data are compared with very low frequency cyclic tests on identical specimens of sand. The comparison indicates that the properties of dry sand are independent of frequency. A simple one-dimensional model of kinematic hardening plasticity is used to predict the dynamic behaviour of the sand. The input parameters for this model are based on the results of static tests. These may be conducted on standard laboratory equipment with only minor modifications. The predictions are in good agreement with the measured data. In particular, the frequency response close to resonance was correctly shown to be asymmetric and the reduction in the resonant frequency with increasing strain amplitude was also correctly represented. The practical consequences of these findings are assessed with regard to soil testing procedures and dynamic analyses of foundations. Particular emphasis is placed on the dynamic analyses of the foundations for vibrating machinery and offshore gravity structures.

KEYWORDS: **damping; resonant column tests; soil properties; stiffness; torsion**

Les propriétés du sable sec de Leighton Buzzard ont été étudiées à l'aide d'un appareil de laboratoire employant une colonne de résonance. Ces données sont comparées avec des essais cycliques de fréquence très basse effectués sur des échantillons identiques du sable. La comparaison indique que les propriétés du sable sec ne dépendent pas de la fréquence. Un modèle très simple unidimensionnel de la plasticité de durcissement cinématique a été employé pour prédire le comportement dynamique du sable, les paramètres d'entrée pour ce modèle étant basés sur les résultats d'essais statiques, qui peuvent s'effectuer sur des appareils normaux de laboratoire avec des modifications de faible importance. Les prédictions s'accordent bien aux données mesurées. En particulier la réponse de fréquence asymétrique près de la résonance et la réduction de la fréquence de résonance avec des amplitudes croissantes de déformation ont été représentées de façon exacte. Les conséquences pratiques de cette étude sont examinées en fonction des procédures pour tester le sol aussi bien que des analyses dynamiques des fondations. On examine plus particulièrement les fondations pour les machines oscillantes et pour les structures gravitationelles au large.

NOTATION

A rotational amplitude
c damping
D damping ratio
k stiffness
K stiffness at zero strain
p' mean effective normal stress
t time
T torque
α total phase of the motion
γ shear strain
θ angular rotation (dots signify time derivative)
θ_y yield rotation
ρ probability density function of yield rotations
σ' mean effective normal stress
τ shear stress
ϕ angle of shearing resistance
ω frequency subscripts d and n denote damped resonant frequency and natural frequency respectively)

Discussion on this Paper closes 2 April 1990. For further details see p. ii.

* University of Cambridge.

INTRODUCTION

The importance of soil dynamics has long been recognized by engineers. However, the role played by the soil in the transmission, dissipation and modification of vibrations is still little understood. Engineers can gain little comfort from codes of practice which generally rely on empirical formulae based on sparse or inappropriate data and inadequate models of soil behaviour. With the advent of large structures whose failure would be environmentally, socially or economically catastrophic increasingly reliable pre-

dictions of dynamic soil behaviour are being demanded at the design stage.

Traditionally engineers have relied on visco-elastic concepts for their predictions of soil behaviour. The equation governing the motion of a viscoelastic system is

$$I\ddot{\theta} + c\dot{\theta} + k\theta = T(t) \tag{1}$$

Equation (1) is a linear second order differential equation with constant coefficients. Virtually all text books that investigate the dynamic behaviour of systems develop solutions to this equation (e.g. Timoshenko *et al.*, 1974). For the case of a harmonic forcing function

$$T(t) = T \cos \omega t \tag{2}$$

and a steady state response of the system (steady state conditions are those that prevail when the response of the system is periodic) the solution to equation (1) is

$$\theta = A \cos (\omega t - \phi) \tag{3}$$

The frequency at which resonance occurs is given by

$$\omega_d = \omega_n \sqrt{(1 - 2D^2)} \tag{4}$$

where the damping ratio

$$D = c/(2\sqrt{(Ik)}) \tag{5}$$

and the undamped natural frequency

$$\omega_n = \sqrt{(k/I)} \tag{6}$$

The phase angle ϕ is given by

$$\phi = \arctan \left| \frac{2D\omega_d/\omega_n}{1 - (\omega_d/\omega_n)^2} \right| \tag{7}$$

In the mid 1950s testing equipment was developed that began to provide data for use in visco-elastic soil models. Hardin & Drnevich (1972a) describe a comprehensive parameter survey based on the results of many tests using different apparatus. Their study suggests that the primary factors affecting the stiffness and damping ratio of a dry sand (the stiffness and damping ratio are the only two soil properties necessary to describe the dynamic behaviour of a soil element of known mass) are

(*a*) strain amplitude
(*b*) mean effective principal stress
(*c*) voids ratio
(*d*) number of strain cycles.

They reported that the frequency of vibration had no effect on the stiffness or damping of sand if these factors (*a*)–(*d*) were held constant. This flatly contradicts the use of visco-elasticity in the analysis of resonant column tests on sand.

Work by Wilson (1985) identified a strong similarity between a truly hysteretic system and the behaviour of soil in a resonant column test apparatus. The words 'truly hysteretic' are used to describe a system in which the load–deformation curve describes a hysteresis loop that is independent of the rate of loading. The equation of motion for such a system is given by

$$I\ddot{\theta} + \mathrm{f}(\theta, \text{sign } (\dot{\theta})) = T(t) \tag{8}$$

The hysteretic restoring torque $\{\mathrm{f}(\theta, \text{sign } (\dot{\theta}))\}$ is an explicit function of the rotation but an implicit function of the angular velocity. The sign of the angular velocity merely indicates loading or unloading. For a truly hysteretic material dynamic testing is unnecessary as the stiffness and damping are independent of the magnitude of either the velocity or acceleration—that is they are independent of frequency. A suitable model encompassing the correct load–deformation characteristics determined from pseudo-static tests should therefore be able to predict the static, cyclic and dynamic behaviour of the material.

With regard to soil, pseudo-static tests would have many advantages over dynamic tests, notably: availability of testing equipment, ease of control and simplicity of logging equipment.

For pseudo-static tests to be accepted as a legitimate method of determining the dynamic properties of soil they must be correlated with dynamic tests. It is the objective of this Paper to provide such a correlation and to introduce a simple, but none the less accurate, model which can predict the dynamic behaviour of the soil within the resonant column apparatus. The predictions of the model are based on the data from pseudo-static tests.

CORRELATION OF DYNAMIC AND STATIC TESTS: ANALYSIS

In order that static and dynamic test data can be compared, a sound theoretical basis must be established.

The inertia of the top cap of the resonant column apparatus used in this study is 107 times greater than that of the soil specimen and so the apparatus can be reduced, for the purposes of mathematical analysis, to that of a single degree of freedom system, with very little error. The inertia of the system is attributable to the top cap while the stiffness and damping are attributable to the soil. There will be some damping due to air resistance on the top cap but this is insignificant compared with the damping of the soil.

The behaviour of a soil is usually described in terms of relationships between the states of stress and strain acting on an element of the soil.

However, for the purpose of comparing the behaviour of geometrically identical specimens of soil this is unnecessary. It is merely sufficient to describe the behaviour in terms common to each test. No attempt has been made here to formulate a relationship between the states of stress and strain within the sample. Instead relationships and comparisons are drawn between the torque applied to the sample and the resulting rotation of the top cap. In turn the rotation of the top cap is geometrically related to the shear strain of the sample at its circumference. This will simplify considerably the mathematics involved in the modelling process and will not require the estimation of stress distributions within the sample.

It will be useful to consider first a basis for the comparison of dynamic and static tests for a visco-elastic system. For such a system with low damping ratios the phase angle at resonance is very close to 90° (from equations (4) and (7) it can be seen that for damping ratios less than 10% the phase angle is greater than 84°. Thus equation (1) can be rewritten at resonance as

$$-I\ddot{\theta} = k\theta$$

$$c\dot{\theta} = T \cos \omega t \tag{9}$$

If the displacement and acceleration amplitudes are measured during a dynamic test conducted at resonance, the ratio of the two would be constant (equation (9)). A graph of the inertial torque component $-I\ddot{\theta}(\max)$ against $\theta(\max)$ for tests with varying input torque amplitudes T would give a straight line of slope k. Consider now a series of static tests. If applied torque is plotted against the corresponding rotation a straight line graph of slope k will result.

It is possible to make some qualitative statements about a hysteretic system that will allow the adoption of an approach similar to the one previously described for a viscous system. The load deformation characteristics of a typical single degree of freedom system are shown in Fig. 1 from which the following statements can be made.

(*a*) When $T = T_{\max}$, $\theta = \theta_{\max}$
(*b*) When $\theta = \theta_{\max}$, $\dot{\theta} = 0$

Minorsky (1947; 1974), Stoker (1950) and Iwan (1967) showed that for a hysteretic system, at resonance, the displacement is very close to harmonic if the forcing function is also harmonic and that the phase angle is approximately 90°. Thus an additional statment can be made.

(*c*) For $T(t) = T \cos \omega t$, $\theta \simeq \theta_{\max} \cos(\omega t - \phi)$ and $\ddot{\theta} = -\ddot{\theta}_{\max}$ when $\theta = \theta_{\max}$

From these three statements equation (8), which is valid at all instants in time, may be used to

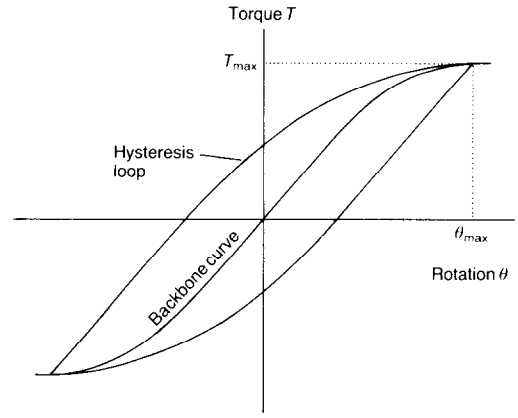

Fig. 1. Load-deformation characteristics of hysteretic system

write

$$-I\ddot{\theta}_{\max} + f(\theta_{\max}) = T \cos \phi \tag{10}$$

for $(\omega t - \phi) = n\pi$, $n = 0, 1, 2 \ldots$
For a phase angle of approximately 90° equation (10) becomes

$$I\ddot{\theta}_{\max} = f(\theta_{\max}). \tag{11}$$

For a pseudo-static load ($\ddot{\theta} \simeq 0$ and $\phi = 0$) equation (10) gives

$$T_{\max} = f(\theta_{\max}) \tag{12}$$

Equations (11) and (12) will form the basis for the comparison of static and dynamic tests. The hysteretic restoring force $f(\theta, \text{sign}(\dot{\theta}))$ will be determined from dynamic tests and compared with the hysteretic restoring force obtained from static tests. If the two hysteretic restoring forces compare well then the soil parameters are unaffected by frequency and the response is governed by equation (8).

The energy dissipation of a system is of considerable importance as it is only through the ability to dissipate energy that vibrations are kept to within tolerable levels. A viscous system will dissipate energy as a result of shearing in a viscous fluid. However, a hysteretic system dissipates energy as a result of the different load–deformation paths for unloading and reloading, resulting from plastic deformations. The energy supplied to a hysteretic system is the area beneath the loading curve and the energy received from the system is the area beneath the unloading curve. The difference between the two is the amount of energy dissipated within the hysteretic system and is proportional to the area of the hysteresis loop. A viscous system will also trace out a

load deformation loop, although the shape of this loop will be frequency dependent. The area of the loop can be related to the damping ratio. Hardin & Drnevich (1972a) give this relationship as

$$D = A_L/(4\pi A_T) \quad (13)$$

where A_L is the area enclosed by the hysteresis loop and A_T is the area enclosed by a triangle the base of which is equivalent to the rotation amplitude and the height to the torque amplitude. Equation (13) will be used to determine the equivalent viscous damping ratio for the soil in the pseudo-static tests. The area of the loop will be the area bounded by the steady-state hysteresis loop.

The energy dissipated in dynamic tests may be determined from the free decay response of the soil column. Steidel (1979) gives the relationship between the amplitude ratio of the nth cycle of the free decay (the ratio of the steady-state strain amplitude to the amplitude of the nth cycle of the free decay) and the damping ratio as

$$D = [1 + \{2\pi n/\ln(\theta/\theta_n)\}^2]^{-1/2} \quad (14)$$

CORRELATION OF STATIC AND DYNAMIC TESTS: RESULTS

Two types of tests have been conducted—static and dynamic. Details of the apparatus are given in Appendix 1. Both types of test used geometrically identical specimens of sand (a solid sample of 38 mm in diameter and 78 mm in height). From the sample geometry it can be shown that the shear strain at the circumference is $\gamma \simeq \theta/4$. In the subsequent discussion of experimental data γ is used in preference to the top cap rotation θ in order to be consistent with published work.

The loading conditions, with the exception of the frequency of the dynamic load, were also identical. The dynamic tests were conducted with an alternating torque over the range 20–120 Hz with resonance typically occurring between 45 and 95 Hz. In comparison the static tests were conducted at a frequency of 0·001 Hz.

Dynamic tests

The inertial torque of the top cap was calculated from the product of the rotational acceleration and the moment of inertia of the top cap. The rotational acceleration was measured using an accelerometer. The inertia had previously been determined by Wilson (1985) and found to be 30×10^{-4} kg . m^2. The accelerometer signal was integrated twice both numerically and electronically to provide displacement data from which the soil shear strain could be calculated. While both methods gave peak strains to within 2% of one another the electronic integrator introduced an erroneous phase shift. Thus, for the purpose of phase calculation numerical integration techniques were used while electronic integration was used to determine the amplitude.

The possibility of the top cap slipping at the soil interface was considered, as this would give erroneous torque–strain characteristics. The acceleration data for a series of tests with increasing strain levels were thoroughly investigated but showed no discontinuous behaviour over the strain range considered in this Paper. If slip was occurring the hysteretic restoring force f(θ, sign ($\dot{\theta}$)) would be discontinuous and the acceleration time history would also exhibit discontinuities. As this did not occur it was assumed that slip was not occurring between the sample and the top cap.

The load–deformation behaviour of the dynamic tests determined in accordance with equation (11) are shown in Fig. 2 and additional details are given in Table 1. For the dynamic tests the ordinate and abscissa of Fig. 2 represent the inertial torque and the strain amplitude respectively. Each point represents a separate test conducted at a different current (torque) amplitude.

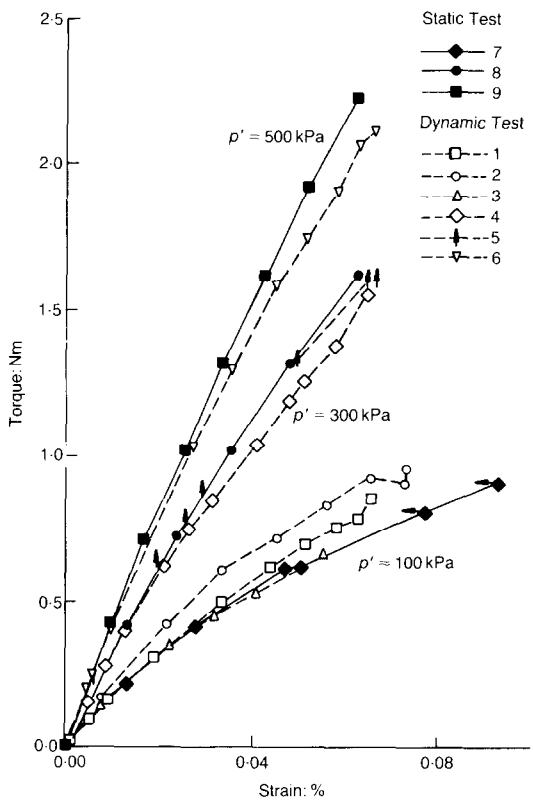

Fig. 2. Static and dynamic torque-strain backbone curves

Table 1. Test results

Test identifier	Cell pressure: kPa	Voids ratio
Dynamic tests		
1	90	0·597
2	93	0·558
3	95	0·625
4	300	0·583
5	300	0·583
6	500	0·578
Static tests		
7	95	0·551
8	300	0·551
9	500	0·551

Furthermore, for a series of tests conducted at the same cell pressure each point represents a different resonant frequency. For example curve number 2 (Fig. 2) has been determined for resonant frequencies varying from 51 Hz at the low strain end to 68 Hz at the high strain end.

Pseudo-static tests

Although the pseudo-static tests were conducted in a different piece of apparatus to that used for the dynamic tests, the boundary conditions of the samples were identical. A torque was applied to the sample by way of a stepper motor and measured with a load cell. The rotation between the two ends of the sample, and hence strain, was measured using an LVDT. The torque and rotation were measured each time the stepper motor was stepped. This gave a considerable number of data points and, consequently, a well-defined series of hysteresis loops.

It was again considered essential to ascertain whether slip was occurring at the soil interface with the top cap. In order to do this a test to failure was conducted and a back analysis performed to show that the shear angle at the interface was sufficient to mobilize the full angle of shearing resistance of the sand, Wilson (1988).

The static tests were characterized by a drifting hysteresis loop which tended to stabilize after a few cycles. These characteristics are shown in Fig. 3 although steady state conditions were not obtained before cessation of this test. The number of load cycles that were required to reach steady state conditions varied considerably although a pattern was observed: the greater the ratio of applied torque to expected yield torque, the greater the number of cycles to achieve steady-state conditions.

The comparison between the load–deformation characteristics for static and dynamic tests is based on equations (11) and (12). From equation (12) it can be seen that for static tests it is not

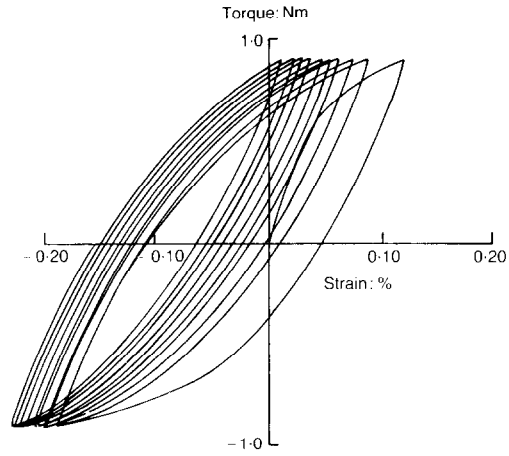

Fig. 3. Development of hysteresis loops for typical static test

necessary to define the complete hysteresis loop but it is only necessary to define the end-points. As the hysteresis loops tended to traverse the strain axis the strain amplitude was taken as one half of the difference between the maximum and minimum strains occurring under steady-state conditions. The results of the static tests are shown with those of the dynamic tests in Fig. 2. There were two tests in which steady state conditions were not reached by the time the test was terminated and these are shown in Fig. 2 as points with a horizontal arrow immediately to their left. The strain amplitude for these points is for the last recorded loop before cessation of the test. The arrow indicates the direction in which the strain amplitude was moving.

Energy dissipation

In Fig. 4 the experimentally determined damping ratios for both the dynamic tests (obtained from the free decay records and equation (14)) and the static tests (measuring the area of the recorded loop and using equation (13)) are plotted for various strain amplitudes.

CORRELATION OF STATIC AND DYNAMIC TESTS: DISCUSSION

The results of the pseudo-static and dynamic tests in Fig. 2 show an extremely good correlation. Any slight discrepancies are considered to be attributable to the different voids ratios of the samples (Table 1) and slight experimental error. From Fig. 2 it is clear that the end-points of the dynamic hysteresis loops and static hysteresis loops for a particular cell pressure lie along a similar backbone curve. It must be remembered

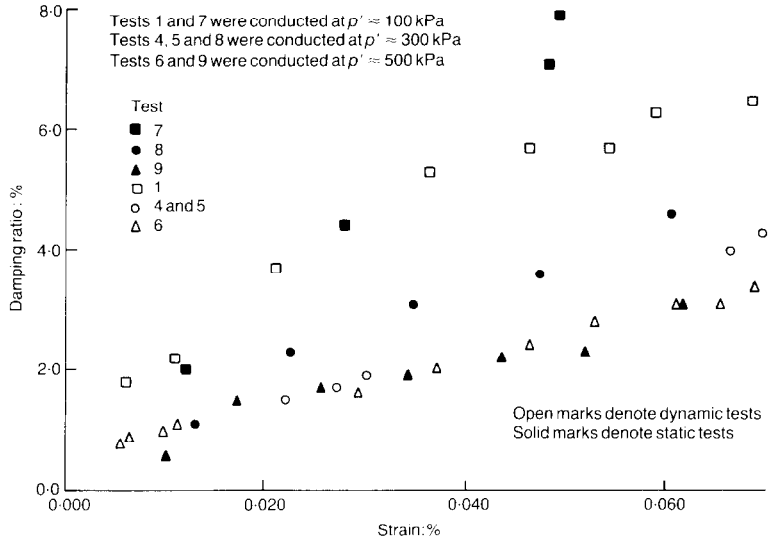

Fig. 4. Static and dynamic damping ratios for dry sand

that the backbone curve is for the steady-state conditions and may be quite different from the virgin loading curve. At stress levels which are low in comparison with failure stress levels, however, steady-state conditions are achieved within several cycles and with little translation along the strain axis: the virgin loading curve and the backbone curve would be similar, therefore.

The tests show that with increasing cell pressure the stiffness increases as expected. The stiffness for a given cell pressure reduces as strain increases, as would be expected. The static and dynamic curves for cell pressures of 300 and 500 kPa appear to diverge with increasing strain but this is merely a reflexion of the different voids ratios and slight experimental error. Hardin & Drnevich (1972b) give an empirical relationship for the variation of the zero strain shear modulus with void ratio. For soils with identical effective stress states the relationship can be written as $G \propto (2{\cdot}973 - e)^2/(1 + e)$. This gives: $G_{e=0{\cdot}55}/G_{e=0{\cdot}58} = 1{\cdot}05$. This compares with an average value from Fig. 2 of 1·07.

Other researchers in this field have also concluded that rate effects are not apparent in sands. Iwasaki *et al.* (1978) tested sands in resonant column and torsional shear apparatuses and found that the shear moduli determined from the two types of test were similar. Their results spanned a range of strain from 0·04 to 0·4% whereas those presented here span 0·0015 to 0·07%.

The static and dynamic measurements of damping ratios in Fig. 4 also correspond quite closely with each other. Both types of test show the same trend of increasing damping ratio with either increasing strain or decreasing effective stress. The relative success of these test correlations supports the proposition that hysteresis in dry sand is strain-rate independent.

HYSTERETIC MODEL FOR RESONANT COLUMN

The inherently hysteretic nature of dry sand has already been established. It has been shown that the soil, for a given strain amplitude, traverses the same hysteresis loop irrespective of the frequency of loading. Thus it is possible to define the hysteresis loop from either static or dynamic tests. In this section a model will be developed that describes the hysteresis loop from static test data. In turn this model will be used to describe the dynamic behaviour of the soil. The dynamic behaviour is represented by the frequency–response characteristics of the soil; the strain amplitude that results from a particular amplitude and frequency of load. It is these characteristics that the model must duplicate.

A number of existing models representing the behaviour of the resonant column were considered. Of these, the most appropriate was a model of kinematic hardening plasticity. This model was greatly simplified in terms of one-dimensional behaviour—torque against top cap rotation. In this form the model is known as a distributed element model. The approach adopted for the solution of this class of model is similar to that of Iwan (1966).

The distributed element model was first pro-

posed by Jenkin (1922) and consists of an ensemble of 'Jenkin' elements, each being composed of a linear spring in series with a frictional slider. Individual elements of the model were treated mathematically by Bernard & Finelli (1953) and independently by Whiteman (1959) and later by Caughy (1960). The distributed element model was treated mathematically by Whiteman (1959) and later Iwan (1966) considered the dynamic behaviour. The model was extended into three dimensions Iwan (1967) and shown, by him, to conform to an advanced kinematic hardening model of plasticity.

An assembly of Jenkin elements will be considered in which the individual elastic springs are of the same stiffness but the frictional sliders slip at different loads. As the assembly is loaded the linear springs extend and the response is elastic. At some extension the load passing through one or more of the springs will reach a level that causes their associated frictional sliders to slip. As extension of the assembly continues, the restoring force from this group of elements will no longer be proportional to the extension but will remain constant at the frictional force of the sliders. Thus for subsequent load increments the stiffness of the assembly will be reduced. This type of behaviour is shown in Fig. 5.

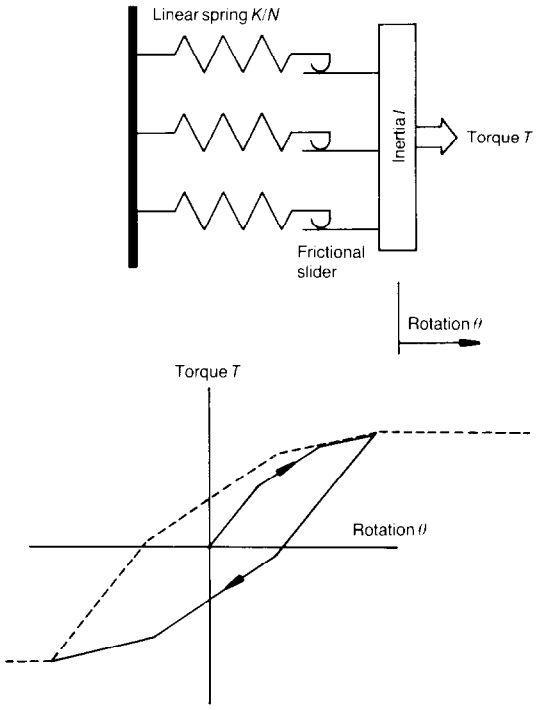

Fig. 5. Distributed element model

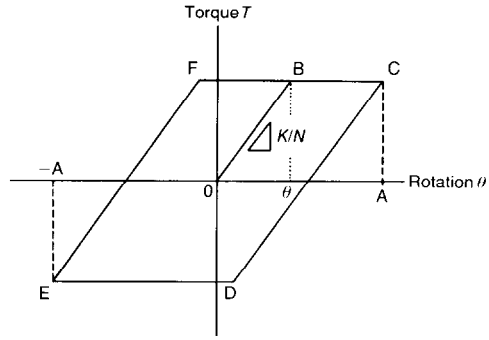

Fig. 6. Characteristics of single Jenkin element

In Fig. 6 the torque–rotation characteristics of an individual element are shown. If the elements are arranged in order of increasing yield rotation then on initial loading (loading along OBC) the restoring torque from the ith element (or a group of elements with identical characteristics) is $t_i = n_i \theta K/N$ for $\theta \leqslant \theta_y$ and $t_i = n_i \theta_y K/N$ for $\theta > \theta_y$. Here, n_i is the number of elements in the ith group and N is the total number of elements.

The total restoring torque for all groups of elements is

$$T = \sum_{i=1}^{q} n_i \theta_y K/N + \sum_{i=q}^{Q} n_i \theta K/N \qquad (15)$$

where q is the number of groups that have yielded (i.e. for which $\theta_y < \theta$) and Q is the total number of groups.

If the number of groups tends to infinity and the rotation at which each slider slips (the yield rotation) varies throughout the assembly in a continuous manner the distribution may be represented in terms of a probability density function ρ of yield rotations (n_i/N against θ_y). Then equation (15) becomes

$$T = K \int_0^{\theta} \theta_y \rho \, d\theta_y + K\theta \int_{\theta}^{\infty} \rho \, d\theta_y \qquad (16)$$

Equation (16) describes the unique backbone curve for a particular hysteretic system characterized solely by the probability density function of yield rotations. The relationship between the function and the backbone curve will be examined below and its use is crucial to the subsequent analysis of the dynamic characteristics of the soil.

By definition the area beneath the probability density function must equal unity and thus the restoring torque equation may be written as

$$T = K\theta\left(1 - \int_0^{\theta} \rho \, d\theta_y\right) + K \int_0^{\theta} \theta_y \rho \, d\theta_y$$

Differentiating both sides with respect to θ

$$\frac{1}{K}\frac{dT}{d\theta} = 1 - \int_0^{\theta} \rho \, d\theta_y \tag{17}$$

The backbone curve may be represented by a polynomial e.g.

$$T = b_0 + b_1\theta + b_2\theta^2 + b_3\theta^3 + \cdots b_n\theta^n \tag{18}$$

Differentiating equation (18) with respect to θ

$$\frac{dT}{d\theta} = b_1 + 2b_2\theta + 3b_3\theta^2 + \cdots nb_n\theta^{(n-1)} \tag{19}$$

Furthermore, the zero strain stiffness is given by

$$K = b_1 \tag{20}$$

Equations (19) and (20) may be substituted into equation (17) and the resulting equation differentiated with respect to θ to give

$$\rho = -2b_2/b_1 - 6b_3\theta/b_1 - \cdots - n(n-1)b_n\theta^{n-2}/b_1 \tag{21}$$

The probability density function of yield rotations has now been described in terms of the backbone curve.

If the assembly is unloaded the unload torque–rotation characteristics may be considered. The restoring torque will be dependent on three sets of elements. One set will consist of all those elements that were elastic at the previous extension, and will therefore still be elastic. Another set will consist of elements that had previously been yielding, but are once again elastic. The final set will consist of those elements that yielded on previous loading and are once again yielding. The restoring torque from the ith group of elements is

$$t_i = n_i\theta K/N \qquad \theta_y \geqslant A$$

$$t_i = n_i\theta K/N - (n_i AK/N - n_i\theta_y K/N) \qquad (A-\theta)/2 < \theta_y < A$$

$$t_i = -n_i\theta_y K/N \qquad -A \leqslant \theta_y < (A-\theta)/2$$

Thus the total restoring torque on unload is

$$T = K\theta\int_A^{\infty}\rho \, d\theta_y + K\int_{(A-\theta)/2}^{A}(\theta - A + \theta_y)\rho \, d\theta_y - K\int_0^{(A-\theta)/2}\theta_y\rho \, d\theta_y \tag{22}$$

$$\text{for} \quad \dot{\theta} < 0 \quad \text{and} \quad -A < \theta < A$$

The method of equivalent linearization of Kryloff & Bogoliuboff (given in English by Minorsky (1947)) may be used to determine the dynamic behaviour of such a model and a summary follows.

A hysteretic system described by equation (8) can be written in an equivalent linear form as

$$I\ddot{\theta} + c\dot{\theta} + k\theta + E(\theta, \dot{\theta}) = A\cos\omega t \tag{23}$$

where the error function $E(\theta, \dot{\theta})$ is given by

$$E(\theta, \dot{\theta}) = f(\theta \text{ sign } (\dot{\theta})) - c\dot{\theta} - k\theta \tag{24}$$

Appropriate values of c and k, the equivalent linearized stiffness and damping parameters, can be found by minimizing the error function. Iwan (1972) considered various minimization criteria and found the minimization of the mean square error to be most appropriate (Appendix 2).

The value of equivalent stiffness and damping is a function of strain amplitude A through the following integral relations

$$\left.\begin{aligned} k &= K(A) \\ c &= C(A)/\omega \end{aligned}\right\} \tag{25}$$

where equations (40) from Appendix 2 give

$$K(A) = \frac{K}{2\pi}\int_0^A (2\beta - \sin 2\beta)\rho \, d\theta_y + K\int_A^{\infty}\rho \, d\theta_y \tag{26}$$

similarly,

$$C(A) = -\frac{K}{\pi}\int_0^A \sin^2\beta \, \rho \, d\theta_y$$

where $\beta = \cos^{-1}(1 - 2\theta_y/A)$.

Equations (26) are applicable to any probability density function. However, if it is assumed that, over the limited range of strains considered here, the backbone curve can be represented by a third order polynomial, equation (21) reduces to

$$\rho = -2b_2/b_1 - 6b_3\theta/b_1 \tag{27}$$

Substituting equation (27) into equations (26) and solving the integral gives

$$\left.\begin{aligned} K(A) &= (b_1 + b_2 A + \tfrac{15}{16}b_3 A^2) \\ C(A) &= \frac{A}{\pi}(2b_3 A + \tfrac{4}{3}b_2) \end{aligned}\right\} \tag{28}$$

Equations (28) in conjunction with equations (25) give the equivalent linear parameters for the hysteretic soil model and thus the resulting frequency response characteristics are governed by the equations for a linear system

$$I\omega^2 = K(A) \pm \left|\left(\frac{T}{A}\right)^2 - C(A)^2\right|^{1/2} \tag{29}$$

and the phase equation

$$\tan\phi = -C(A)/(K(A) - I\omega^2).$$

Resonance occurs when the two roots of the frequency response equation are equal. That is when the radical becomes

$$I\omega^2 = K(A) \tag{30}$$

Substituting this result into the phase equation gives

$$\phi_{\text{resonance}} = \pi/2 \tag{31}$$

The equivalent viscous damping ratio for the soil system may be obtained by substituting equations (25) and (30) into (5) to give

$$D = \frac{1}{2}\frac{C(A)}{K(A)} = \frac{A}{\pi}\frac{(b_3 A + \frac{2}{3}b_2)}{(b_1 + b_2 A + \frac{15}{16}b_3 A^2)} \tag{32}$$

EVALUATING $K(A)$ AND $C(A)$

In order to evaluate $K(A)$ and $C(A)$ the backbone curve will be described in terms of a third order polynomial (equation (21)). The results from the static test 9 (Fig. 2 and Table 1 give details of the tests) were used to determine a best-fit cubic for the tests conducted at a cell pressure of 500 kPa. The equation was found to be

$$T = 1{\cdot}1 \times 10^3\theta - 102 \times 10^3\theta^2 + 676 \times 10^4\theta^3$$

where $\theta = 4\gamma$. For a cell pressure of 300 kPa the results for static test 8 gave

$$T = 8{\cdot}97 \times 10^2\theta - 124 \times 10^3\theta^2 + 116 \times 10^5\theta^3$$

There were insufficient data points from static test 7 to fit a cubic curve and so the curve from dynamic test 1 was used. It was felt that this curve was a reasonable fit to all the low effective stress data. The resulting equation was found to be

$$T = 4{\cdot}8 \times 10^2\theta - 101 \times 10^3\theta^2 + 156 \times 10^5\theta^3$$

From these equations the equivalent linear parameters may be determined in accordance with equation (28) and equation (29) may be used to determine the frequency response of the system.

COMPARING MODEL PREDICTIONS AND TEST RESULTS

The frequency–response characteristics of the model can be determined from equation (29). The predictions of the model are compared with the results of frequency-response tests in Figs 7–9. From this comparison it can be seen that the model embodies the essential characteristics of the soil behaviour observed in the tests. These essentials are the dependence of the resonant frequency on strain amplitude and the rapid increase in strain below resonance for a very small increase in frequency. This latter point is similar to the jump phenomenon observed in a Duffing type strain-softening spring (Stoker (1950)).

With regard to the variation in the resonant frequency with shear strain amplitude both the

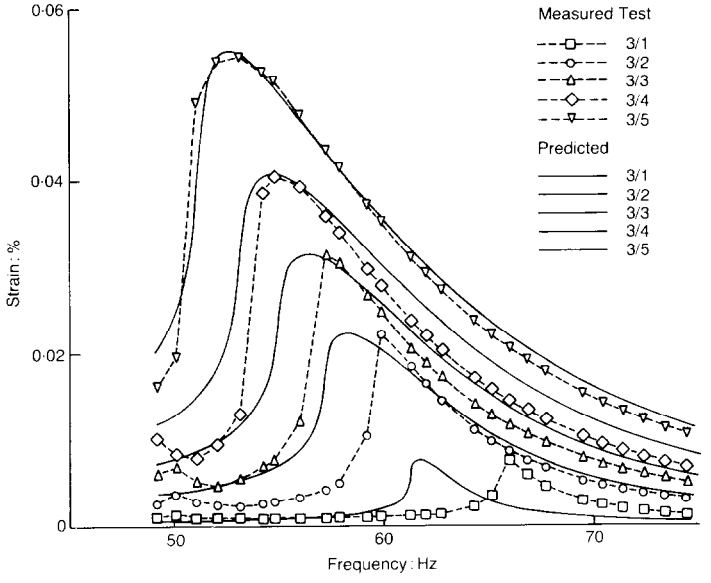

Fig. 7. Measured and predicted dynamic response: test 3, $p' = 95$ kPa

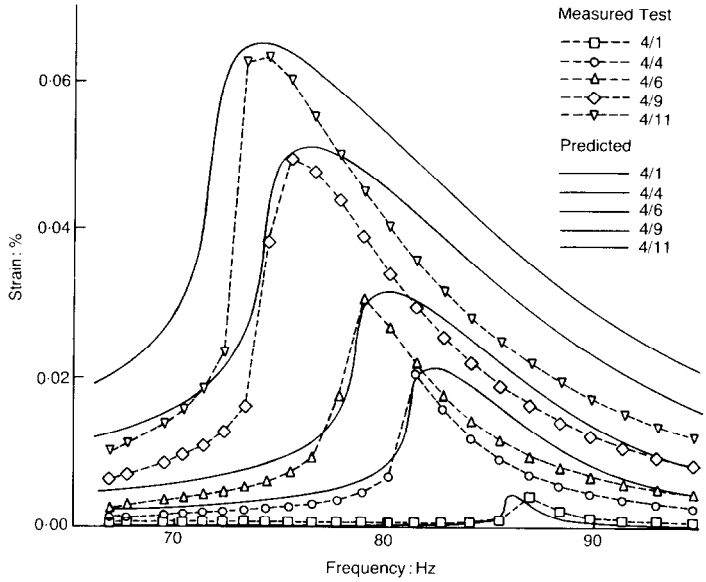

Fig. 8. Measured and predicted dynamic response: test 4, p' = 300 kPa

model data and the experimental data show that it is still significant at shear strain amplitudes below 0·01%. This contradicts a commonly held view that soil can be regarded as linear elastic at such small strains and agrees with the findings of Iwasaki *et al.* (1978).

The characteristics of the soil identified in the resonant column are not particular to that piece of apparatus but have also been observed in many reported field tests e.g. those of Fry reported by Richart & Whitman (1967), Lorenz (1953) and others.

The damping ratios determined experimentally from the dynamic tests, and predicted from the static tests, are shown in Fig. 10. The predicted damping ratios are extremely close to the mea-

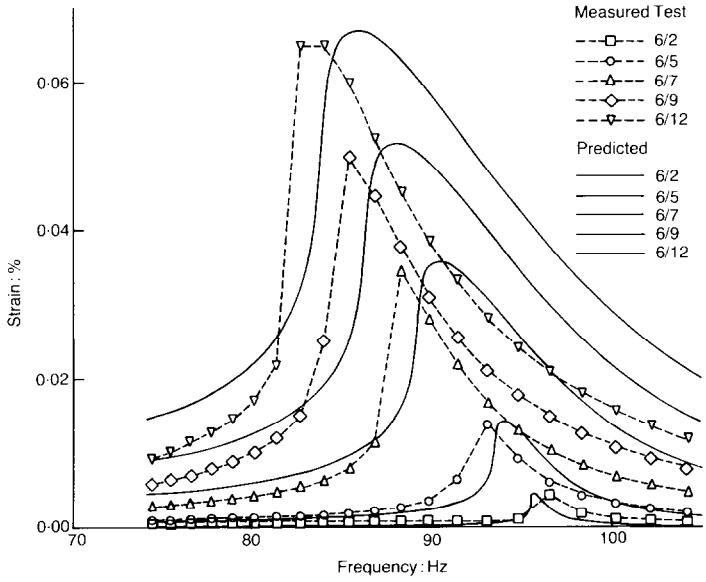

Fig. 9. Measured and predicted dynamic response: test 6, p' = 500 kPa

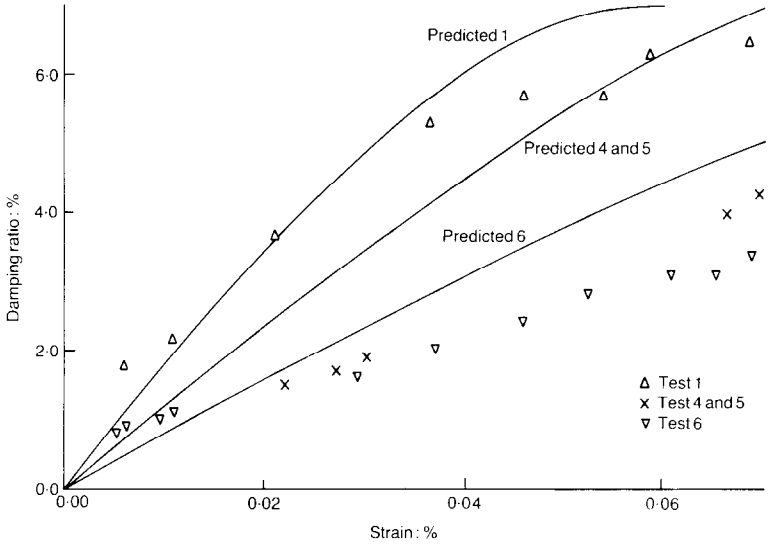

Fig. 10. Dynamic damping ratio: measured and predicted

sured values for test 1. Although the predictions for the 300 and 500 kPa tests do not show such a good fit they will almost certainly be good enough for practical purposes.

PRACTICAL CONSEQUENCES

The most obvious practical consequence of this work is the possibility of predicting the results of dynamic tests from static test data. This is discussed further in the conclusion to this Paper. Equally significant is the rapid increase in soil strain that occurs below resonance for a very small increase in the frequency of applied load. This phenomenon could certainly lead to serviceability failures of sensitive foundation installations. The designer must not only concern himself with the resonant frequency of the soil–structure system but also with the variation of the resonant frequency with strain. In this respect it must be remembered that the variation of the resonant frequency is apparent even at small strain amplitudes.

It is perhaps useful to consider some practical instances of steady state loading conditions and the effects of the response phenomenon described here. The steady state conditions are defined as those prevailing while the soil is repeatedly traversing the same hysteresis loop (i.e. once any initial particle rearrangement has taken place and when a continuously repeating change in the soil fabric is occurring). It should be remembered that steady state conditions will occur after relatively few load cycles.

Firstly consider the response of a machine foundation to vibrations introduced as a result of its operation. Generally the amplitude of the load may be expected to increase as the frequency of the vibrations increase. Under working conditions the frequency of the induced load will either be above or below the resonant frequency of the soil–structure system. If it is below, the designer should bear in mind the migration of the resonant frequency to that of the loading frequency with increasing soil strain. Should resonance occur the effects would be dramatic with an almost instantaneous increase in soil strains (a fourfold increase in strain amplitude was observed experimentally for only a 1% increase in the frequency of loading). Cyclic rotations of the order of 1/1000 may be intolerable for sensitive foundations or machines. They could also lead to an alteration in the arrangement of soil particles and thereby to excess pore pressures in saturated soils or to compaction and settlement following drainage. If, on the other hand, the machine vibration is at a frequency above the resonant frequency of the soil–structure system (a wholly undesirable but sometimes unavoidable situation) the designer must appreciate that during start up the machine will pass through a condition of resonance. However, the actual response of the soil–structure will almost certainly be less severe than that predicted from a visco-elastic analysis of the foundation. This is a result of the reducing natural frequency of the foundation and the increasing frequency of the load as resonance is passed.

Secondly consider the response of an offshore gravity structure. For this type of structure, pre-

dominantly under wave loading, the amplitude of the load increases as the frequency of the load decreases. As a result it is feasible that the frequency of maximum load and the resonant frequency of the soil–structure system will traverse the same path. In any event the loading frequency will not diverge from the resonant frequency of the soil–structure as much as would be suggested from a visco-elastic analysis. Typically, for the northern North Sea, the wave energy may be expected to increase from a minimum at around 0·2 Hz to a maximum at around 0·05 Hz (Hallan, Heaf & Wootton, 1978). The zero strain resonant frequency of an offshore gravity structure may be expected to be about 0·5 Hz decreasing with increasing strain to about 0·2Hz (Hallan, Heaf & Wootton, 1978). One might therefore expect existing structures to be safe, but a thorough analysis of elasto-plastic foundation behaviour is justified.

CONCLUSION

The first part of this Paper was concerned with a comparison between static and dynamic torsional tests on dry sands. It was shown that for soil strains of up to 0·07%, steady-state conditions, and various loading frequencies between 0·001 and 120 Hz, the behaviour of the soil is independent of the frequency of applied load. In the second part of the Paper a simple but accurate model for the behaviour of soil in the resonant column apparatus was developed, based on the results of static tests. It was shown that for the class of model adopted, that of kinematic hardening plasticity, the predictions were in good agreement with the experimental data. Dynamic tests on dry sands may therefore be considered unnecessary.

It was quite clearly shown that the steady-state frequency response characteristics can be determined from a knowledge of the backbone curve. The backbone curve can be defined from just the end-points of the hysteresis loop and further details of the loop are unnecessary for a simple analysis. Thus a standard triaxial cell in which a torsional load is applied first in one direction and then the other will, after sufficient load reversals, give the end-points of the steady state hysteresis loop.

However, one must recognize the limitations of these results, notably: the range of strains covered, the soil being restricted to dry sands, and the steady-state conditions. With regard to the dry nature of the soil Wilson (1985) presented results that showed there to be little difference between the response characteristics of dry or water-saturated sands over a similar strain and frequency range. It may be assumed that the results presented would also be unaffected by the presence of pore water, at least for the moderate frequencies of excitation used in this study.

The comparison between static and dynamic behaviour and the model predictions are only applicable to steady-state conditions and not transient conditions. Transient loading conditions such as explosions and transient soil states such as cyclic mobility or liquefaction are beyond the scope of this work. However, it must be remembered that steady-state conditions can exist after several load cycles and so apparently transient loads such as earthquakes may well be within the scope of this work.

APPENDIX 1. TEST APPARATUS AND PROCEDURES

Dynamic tests

The resonant column rig was designed by K. H. Stokoe (University of Texas) and built at Cambridge University. A description follows which should be read in conjunction with Fig. 11

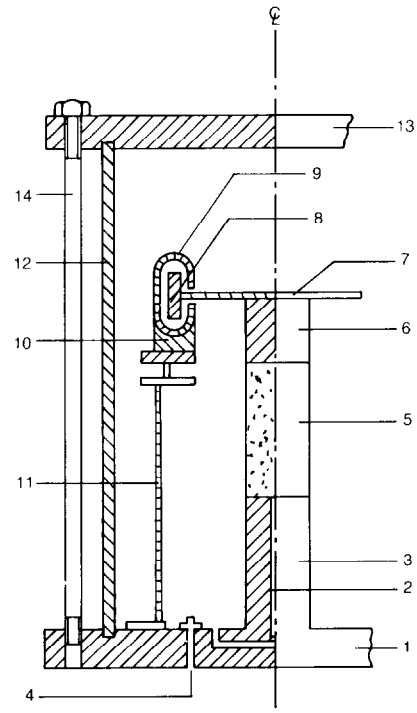

1 Base
2 Pore pressure line
3 Lower platen
4 Compression fitting
5 Sample
6 Top cap
7 Moving cruciform
8 Permanent magnets
9 Electrical coils
10 Holding ring
11 Outer sleeve
12 Pressure sleeve
13 Closing plate
14 Tension bolts

Fig. 11. Stokoe apparatus

(numbers enclosed in ( ) refer to component numbers in Fig. 11).

The sample (5) is placed on a lower platen (3), a top cap (6) closes the upper end of the sample. An outer sleeve (11) is placed over the sample and carries the coil assembly (9, 10). The moving cruciform (7) is rigidly connected to the top cap and with it forms the active platen. A pressure sleeve (12) surrounds the complete assembly. A lid (13) closes, and is brought into firm contact with the pressure sleeve by tightening the tension bolts (14). By passing a current through the driving coils (9) a force is exerted on the permanent magnets (8) and results in the movement of the active platen.

The resonant column apparatus was used for two types of test—frequency response tests and free decay tests. All tests were computer controlled and logged.

The frequency response tests were concerned with establishing the general dynamic behaviour of the soil and the soil's resonant frequency. A fixed amplitude torque was applied to the sample at various frequencies. The frequencies at which the torque was applied increased in 1 Hz steps from 20 to 110 Hz. A thousand cycles of torque were applied at each frequency and the response of the soil to the last 100 cycles of each frequency was recorded at a rate of 32 times the test frequency. The response of the soil was measured by way of an accelerometer placed on the top platen assembly. The acceleration signal was both numerically (using the Newark beta method) and electronically double integrated to obtain displacement and thus strain. Accelerometers were placed on the lower platen to check that it remained quiescent during all testing. The alternating current driving the apparatus was also recorded throughout the test at a frequency of 32 times the test frequency. The frequency response tests were conducted at a number of torque amplitudes.

The free decay tests were conducted in order to obtain a measure of the damping of the soil. A thousand cycles of torque were applied at the resonant frequency. After the last cycle the control program placed the driving circuit into open circuit mode and the amplitude of vibration of the soil column decayed to quiescence. The control program recorded the decay of the vibrations. Recording started at the finish of the 995th load cycle.

Pseudo-static tests

The pseudo-static test apparatus has been designed and built at Cambridge University and is known as the 'Wilson rig'. The Wilson rig has been used to test solid samples under a variety of total load and effective stress conditions. The rig is computer controlled and logged. Both load and strain controlled tests are possible. A diagram of the version of the rig used for the tests reported here is shown in Fig. 12. In the following description of the rig the numbers in ( ) refer to the component numbers in Fig. 12.

The sample (1) was prepared on the lower platen (2) which incorporated a torsional load cell (3). The upper end of the sample was closed by a top cap (4) which was, in turn, rigidly connected to the top platen assembly (5). The mass of the top platen assembly was identical to that of the resonant column apparatus. The bearings (6) on the top platen assembly permitted vertical movement but not rotational movement. A torque was applied to the lower platen by the stepper motor (7). Rotation of the sample was measured via an LVDT (8). The LVDT body was rigidly fixed to the top cap while the LVDT core was rigidly attached to the lower platen. Thus any flexibility of the apparatus or stepper motor gearbox had no effect on the measured strain (rotation) of the

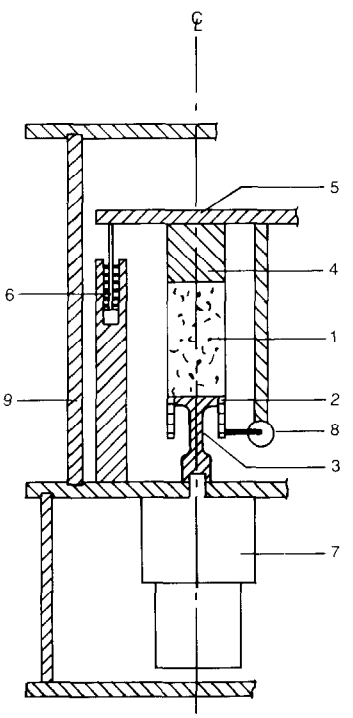

1 Sample
2 Lower platen
3 Load cell
4 Top cap
5 Top platen assembly
6 Bearings
7 Stepper motor
8 LVDT
9 Pressure sleeve

Fig. 12. Wilson apparatus

sample. Both the upper and lower platens of the Wilson rig were made of the same materials and machined in the same way as those of the resonant column apparatus.

In order to replicate the conditions present in the resonant column, load controlled tests were performed. The computer control program stepped the motor in one direction (each step of the motor corresponded to a strain of approximately 0·001%; the motor could also be used in half step mode). The input and output voltages from the LVDT and load cell were averaged over 1 s and recorded. The averaging started 1 s after the motor had been stepped. All data was recorded to 12 bit accuracy (an accuracy better than 0·025% of full-scale deflexion). Once the required torque level had been reached the control program reversed the motor. This process was continued for a user-specified number of cycles. The control program forms part of the DYNAST (DYNamic And STatic) soil testing suite of programs that manage all aspects of the resonant column and torsional column testing at Cambridge including the control, data gathering, data reduction and report preparation for tests.

APPENDIX 2

The minimization of the mean square error term given in equation (24) takes the following form (the bar denotes the time average)

$$\frac{\partial}{\partial k}\overline{\{E(\theta, \dot{\theta})^2\}} = \frac{\partial}{\partial c}\overline{\{E(\theta, \dot{\theta})^2\}} = 0$$

These conditions give

$$\overline{\dot{\theta}E(\theta, \dot{\theta})} = \overline{\theta E(\theta, \dot{\theta})} = 0$$

Substituting for $E(\theta, \dot{\theta})$, referring to equation (24)

$$\overline{c\dot{\theta}^2} + \overline{k\theta\dot{\theta}} - \overline{\dot{\theta}\mathrm{f}(\theta, \mathrm{sign}\,(\dot{\theta}))} = 0$$

$$\overline{k\theta^2} + \overline{c\theta\dot{\theta}} - \overline{\theta\mathrm{f}(\theta, \mathrm{sign}\,(\dot{\theta}))} = 0$$

There can be written (noting that for any stationary random process that is differentiable $\overline{\theta\dot{\theta}} = 0$)

$$c = \overline{\dot{\theta}\mathrm{f}(\theta, \mathrm{sign}\,(\dot{\theta}))} \cdot \overline{(\dot{\theta}^2)^{-1}}$$

$$k = \theta\mathrm{f}(\theta, \mathrm{sign}\,(\dot{\theta})) \cdot \overline{(\theta^2)^{-1}} \qquad (33)$$

If an assumption is now made that

$$\theta = A\cos\alpha \qquad (34)$$

where $\alpha = \omega t - \phi$, the total phase of the motion (Minorsky (1947)) shows that the time average can be replaced by the average over one cycle ($\alpha = 0$ to 2π). Thus

$$\bar{\theta}^2 = \frac{1}{2\pi}\int_0^{2\pi}(A\omega\sin\alpha)^2\,\mathrm{d}\alpha = \frac{(A\omega)^2}{2}$$

$$\bar{\theta}^2 = \frac{1}{2\pi}\int_0^{2\pi}(A\cos\alpha)^2\,\mathrm{d}\alpha = \frac{A^2}{2} \qquad (35)$$

Substituting equations (34) and (35) into (33) gives the equivalent linearized parameters as

$$c = \frac{-1}{\pi A\omega}\int_0^{2\pi}\mathrm{f}(A\cos\alpha, \mathrm{sign}\,(-\omega A\sin\alpha))\sin\alpha\,\mathrm{d}\alpha$$

$$k = \frac{1}{\pi A}\int_0^{2\pi}\mathrm{f}(A\cos\alpha, \mathrm{sign}\,(-\omega A\sin\alpha))\cos\alpha\,\mathrm{d}\alpha \qquad (36)$$

These equations may be written more conveniently as

$$k = K(A)$$

$$c = C(A)/\omega \qquad (37)$$

where

$$K(A) = \frac{1}{A\pi}\int_0^{2\pi}\mathrm{f}(A, \alpha)\cos\alpha\,\mathrm{d}\alpha$$

$$C(A) = \frac{-1}{A\pi}\int_0^{2\pi}\mathrm{f}(A, \alpha)\sin\alpha\,\mathrm{d}\alpha \qquad (38)$$

The hysteresis loop of the distributed element model is symmetric and so $K(A)$ may be evaluated between the limits of 0 and π. Substituting equation (22) into equation (12) gives an expression for the function f in terms of the static data. The resulting expression may be substituted into equations (38) giving

$$K(A) = \frac{2}{A\pi}\int_0^{\pi}\left|K\theta\int_A^{\infty}\rho\,\mathrm{d}\theta_y + K\int_{(A-\theta)/2}^{A}(\theta - A + \theta_y)\rho\,\mathrm{d}\theta_y - K\int_0^{(A-\theta)/2}\theta_y\rho\,\mathrm{d}\theta_y\right|\cos\alpha\,\mathrm{d}\alpha \qquad (39)$$

A similar expression is obtained for $C(A)$.

If, for the time being, it is assumed that ρ is unknown, a general solution to equation (39) may be found by reversing the order of integration and integrating first with respect to α e.g.

$$K(A) = \frac{K}{2\pi}\int_0^{A}(2\beta - \sin 2\beta)\rho\,\mathrm{d}\theta_y + K\int_A^{\infty}\rho\,\mathrm{d}\theta_y \qquad (40)$$

similarly,

$$C(A) = -\frac{K}{\pi}\int_0^A \sin^2\beta\ \rho\ \mathrm{d}\theta_y$$

where $\beta = \cos^{-1}(1 - 2\theta_y/A)$.

REFERENCES

Bernard, R. K. & Finelli, J. (1953). *Pilot studies on soil dynamics* Special Technical Publication 156, Philadelphia: Am. Soc. Testing Materials.

Bolton, M. D. (1986). The strength and dilatancy of sands. *Géotechnique* **36,** No. 1, Mar., 65–78.

Caughy, T. K. (1960). Sinusoidal excitation of a system with bilinear hysteresis, *Trans. Am. Soc. Mech. Engng* **27,** 640–643.

Hallan, M. G., Heaf, N. J. & Wootton, L. R. (1978). *Dynamics of marine structures: methods of calculating the dynamic response of fixed structures subject to wave and current action.* Report UR8 2nd Edn Atkins Research and Development/CIRIA Underwater engineering group, London: Atkins/Construction Industry Research and Information Association.

Hardin, B. O. & Drnevich, V. P. (1972a). Shear modulus and damping in soils: measurement and parameter effects. *J. Soil Mechs Div. Am. Soc. Civ. Engrs*, **98,** SM6, June, 603–624.

Hardin, B. O. & Drnevich, V. P. (1972b). Shear modulus and damping in soils: design equations and curves. *J. Soil Mechs Div. Am. Soc. Civ. Engrs*, **98,** SM7, July, 667–692.

Iwan, W. D. (1966). A distributed element model for hysteresis and its steady state dynamic response. *J. Applied Mechs, Am. Soc. Mech. Engng* **88,** Series E, No. 4 893–900.

Iwan, W. D. (1967). On a class of models for the yielding behaviour of a continuous and composite system. *J. Appl. Mechs Am. Soc. Mech. Engng.* **89,** Series E, No. 3 612–617.

Iwan, W. D. & Patula, E. J. (1972). The merit of different error minimization criteria in approximate analysis. *J. Appl. Mechs, Am. Soc. Mech. Engng* **94,** Series E, No. 1, 257–262.

Iwasaki, T., Tatsuoka, F. & Yoshikazu, T. (1978). Shear moduli of sands under cyclic torsional shear loading. *Soils and Fdns*, **18,** No. 1.

Jenkin, C. F. (1922). A mechanical model illustrating the behaviour of metals under static and alternating loads. *Engineering*, **114,** (CXIV) 603.

Lorenz, H. (1953). *Elasticity and damping effects of oscillating bodies on soil.* Am. Soc. Testing Materials Special Technical Publication 156, Philadelphia: ASTM.

Minorsky, N. (1947). *Introduction to non-linear mechanics.* Michigan: Ann Arbor.

Minorsky, N. (1974). *Nonlinear oscillations.* New York: Robert E. Krieger Publishing.

Richart, F. E. & Whitman, R. V. (1967). Comparison of footing vibration tests with theory. *J. Soil Mechs, Am. Soc. Civ. Engrs* SM6, Nov. 143–168.

Steidel, R. F. (1979). *An introduction to mechanical vibrations* 2nd Edn, New York: Wiley.

Stoker, J. J. (1950). *Nonlinear vibrations.* New York: Interscience Publishers.

Timoshenko, S., Young, D. H. & Weaver, W. (1974). *Vibration in engineering.* New York: Wiley.

Whiteman, I. R. (1959). A mathematical model depicting the stress–strain diagram and the hysteresis loop. *J. Appl. Mechs, Am. Soc. Mech. Engng* **81,** No. 1, 95–100.

Wilson, J. M. R. (1985). *The dynamic properties of soil.* M Phil dissertation, Engineering Department, Cambridge University.

Wilson, J. M. R. (1988). *An experimental and theoretical investigation into the dynamic behaviour of soils.* PhD dissertation, Engineering Department, Cambridge University.